Ingress of Coolant Event simulation with TRACE code with accuracy evaluation and coupled DAKOTA Uncertainty Analysis

Ingress of Coolant Event simulation with TRACE code with accuracy evaluation and coupled DAKOTA Uncertainty Analysis

Andrea Bersano[a], Fulvio Mascari[b], Maria Teresa Porfiri[c], Pietro Maccari[d], Cristina Bertani[a]

[a] Politecnico di Torino, Energy Department, Corso Duca degli Abruzzi 24, 10129, Turin, Italy
[b] ENEA C.R. Bologna, FSN-SICNUC, Via Martiri di Monte Sole 4, 40129, Bologna, Italy
[c] ENEA C.R. Frascati, UTFUS, Via Enrico Fermi 45, 00044 Frascati, Rome, Italy
[d] University of Bologna, Industrial Engineering Department, Viale del Risorgimento 2, 40129, Bologna, Italy

Corresponding authors:
Andrea Bersano
andrea.bersano@polito.it
Politecnico di Torino, Corso Duca degli Abruzzi 24, 10129, Turin, Italy

Fulvio Mascari
fulvio.mascari@enea.it
ENEA C.R. Bologna, FSN-SICNUC, Via Martiri di Monte Sole 4, 40129, Bologna, Italy

Abstract
Among the Postulated Initiating Events in nuclear fusion plants, the Ingress of Coolant Event (ICE) in the Plasma Chamber is one of the main safety issues. In the present paper, the best estimate thermal-hydraulic system code TRACE, developed by USNRC, has been adopted to study the ICE, and it has been qualified based on experimental results obtained in the Integrated ICE facility at JAERI. A nodalization has been developed in the SNAP environment/architecture, using also the TRACE 3D Vessel component where multidimensional phenomena could occur. The accuracy of the code calculation has been assessed both from a qualitative and quantitative point of view. In addition, an Uncertainty Analysis (UA), with the probabilistic method to propagate the input uncertainties, has been performed to characterize the dispersion of the results. The analysis has been carried out with the DAKOTA toolkit coupled with TRACE code in the SNAP environment/architecture. Results show the adequacy of the 3D nodalization and the capability of the code to follow the transient evolution also at a very low pressure. Response correlations have been computed to characterize the correlation between the selected uncertain input parameters and the Plasma Chamber pressure.

Keywords: Ingress of Coolant Event; TRACE; Code accuracy; FFTBM; DAKOTA; Probabilistic method to propagate the input uncertainty

Abbreviations

AA	Average Amplitude
CDF	Cumulative Distribution Function
CHF	Critical Heat Flux
FFTBM	Fast Fourier Transform based Method
FOM	Figure Of Merit
ICE	Ingress of Coolant Event
JAERI	Japan Atomic Energy Research Institute
LOCA	Loss Of Coolant Accident
LWR	Light Water Reactor
MV	Magnetic Valve
PC	Plasma Chamber
PDF	Probability Density Function
PFC	Plasma-Facing Components
PhW	Phenomenological Window
RP	Relief Pipe
RTA	Relevant Thermal-hydraulic Aspects
RTP	Relevant Thermal Hydraulic Phenomena
SD	Simulated Divertor
SNAP	Symbolic Nuclear Analysis Package
SOT	Start Of the Transient
ST	Suppression Tank
TRACE	TRAC/RELAP Advanced Computational Engine
UA	Uncertainty Analysis
USNRC	US Nuclear Regulatory Commission
VV	Vacuum Vessel
WF	Weighted Frequency

1. Introduction

In the medium-long term, nuclear fusion is expected to become a viable energy source from the technical and economical point of view. A huge R&D effort is conducted worldwide for the exploitation of this promising energy source that presents several technical challenges. A relevant aspect to be addressed is the safety of fusion reactors that present different issues with respect to the fission ones.

In the frame of the safety assessment, the need to validate the computer codes available for the fission nuclear power plant has been highlighted. The scope is to extend their applicability in the fusion context.

The selection of the accident analyses typical for the fusion facilities [1] showed that the in Vacuum Vessel (VV) Loss Of Coolant Accident (LOCA) is, among them, one of the most important; the in-vessel LOCA is also called Ingress of Coolant Event (ICE). The ICE in the Plasma Chamber (PC) in case of a break of the cooling tubes installed in the Plasma-Facing Components (PFCs) leads to the loss of vacuum in the PC and a consequent pressurization of the PC and the VV due to the flashing of liquid water in a low pressure environment. In order to mitigate the over-pressure in the PC and in the VV a relief pipe connects the VV to a Suppression Tank (ST) that reduce the pressure avoiding structural damages.

The integrated ICE facility was built at JAERI (Japan Atomic Energy Research Institute – Naka Laboratories) to reproduce the thermal-hydraulic behavior of this accident. The facility scaling factor is 1/1600 with respect to ITER FEAT [2] design for all the major components (volume of PC, break size, injected water volume, flow area of the divertor throat, relief pipe diameter and water volume in the ST) [3].

Several efforts have been devoted to the analyses of the capability of different computer codes for the simulation ICE in fusion like devices. For thermal-hydraulic codes examples are reported in [4] and [5] respectively for RELAP5 and TRAC; for severe accident codes examples are reported in [6] and [7] respectively for MELCOR and ASTEC; for fast-running codes an example is reported in [8] for CONSEN.

In the past, to support the independent vendor review of Light Water Reactor (LWR) fission designs, the US Nuclear Regulatory Commission (USNRC) maintained four separate computer codes (RAMONA, RELAP5, TRAC-B and TRAC-P) to analyze the system thermal-hydraulic response [9]. Over the last years, the USNRC has developed an advanced best-estimate thermal-hydraulic system code, by merging, among other things, the capability of the previous codes into a single code. This new code is called TRAC/RELAP Advanced Computational Engine or TRACE [10]. It is a component-oriented code designed to perform best-estimate analyses for LWR. Considering its advanced thermal-hydraulic capability and the possibility to run at water pressure between 0.001 Pa and $99.99999*10^6$ Pa [10], it can be used also to simulate transient progression of interest for the safety of fusion plant.

In the present paper, the ICE is simulated with TRACE code and the results are compared to the experimental data obtained in ICE facility. A TRACE nodalization has been developed by using the Symbolic Nuclear Analysis Package (SNAP) [11], and the 3D Vessel component has been used to simulate the components where multidimensional phenomena could take place. The accuracy of the code calculation has been evaluated both from the qualitative and quantitative point of view [12]. The Phenomenological Windows (PhWs) and the related Relevant Thermal-hydraulic Aspects (RTAs) have been identified and the code qualitative capability to reproduce the experimental results is evaluated with subjective marks. Then, to assess the code accuracy, a quantitative evaluation has been performed using the Fast Fourier Transform based Method (FFTBM) [13].

Finally, a first Uncertainty Analysis (UA) has been carried out to characterize the dispersion of the results and the relationship between some selected uncertain input parameters on the output parameter, the PC pressure, selected as a Figure Of Merit (FOM). Among the possible methodologies developed for UA, the probabilistic propagation of input uncertainty through the code [14] has been

adopted. The method has been applied using the DAKOTA toolkit [15] coupled with TRACE in the SNAP environment/architecture.

2. *Description of ICE test facility and experimental conditions*

2.1 Description of ICE facility

The Integrated ICE facility [3] at JAERI is a scaled-down experimental test facility used to thermal-hydraulically characterize two-phase flow during an ICE in ITER reactor. As reported in [3] the general scaling factor against the ITER FEAT design is of 1/1600. The PC is a horizontal cylinder with an inner diameter of 0.6 m and a length of 2.1 m for a volume of 0.6 m^3. The VV is a horizontal cylinder with an inner diameter of 0.5 m and a length of 1.72 m for a volume of 0.34 m^3. The PC is connected to the VV by a Simulated Divertor (SD), a rectangular metal frame 0.162 m thick, 0.12 m width and 1.2 m length. The SD simulates ITER divertor cassettes. The frame has 12 evacuation slits (width 5 mm, length 80 mm each) that look like the spaces among the cassettes. Images of the facility and of the SD can be found in [5].

The rupture of the cooling tubes is simulated in the facility by the injection of water through 3 nozzles (diameter 10 mm) connected to a pressurized boiler with electrical heaters. The maximum temperature achievable in the boiler is 523.15 K and the maximum pressure is 4 MPa.

The bottom of the VV is connected to a Relief Pipe (RP), with a diameter of 49.5 mm, that drives the fluid to the ST aimed at reducing the pressure in the PC and in the VV in case of an ICE. Along the RP a Magnetic Valve (MV) that opens at a fixed PC pressure set-point models the rupture disks of the ITER design [5]. The RP is connected to the ST, a vertical cylinder with an inner diameter of 0.8 m and a height of 1.96 m for a total volume of 0.93 m^3. In the ST water is stored, with an initial water volume lower than 0.5 m^3 [5]; the RP outlet is under the water surface for steam bubbling to enhance the condensation. A schematic drawing of the integrated ICE facility is shown in Fig. 1 with its main dimensions.

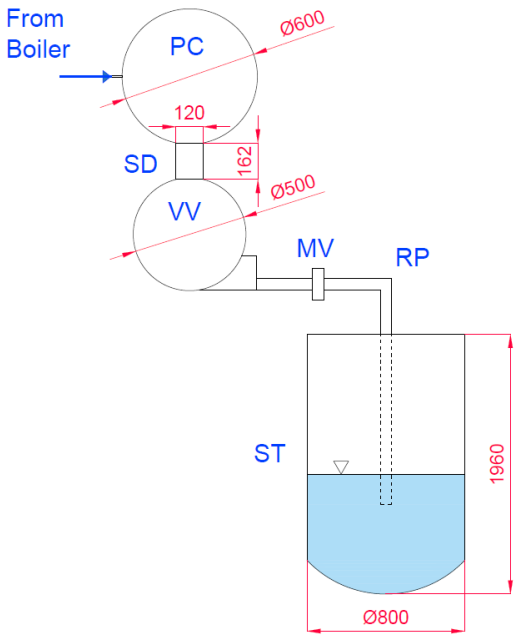

Fig. 1. Schematic view of the integrated ICE facility [16]

2.2 Description of the selected test

Among the tests performed in ICE facility [16][17], it has been chosen Case4 of the experimental campaign performed in March 2000, since it presents a relatively long water injection. In this test, 2 out of 3 nozzles are used for an injection time of 45 s and the PC and VV heaters are turned off at the beginning of the transient. Table 1 presents the main parameters of the selected transient and the facility system initial conditions.

In the experimental data available to the authors, the water injection starts after 10 s from t=0 s. The pressurization of the PC and of the VV is fast (around 0.46 MPa in 10 s) and limited by the activation of the ST as far as the PC pressure exceeds 0.15 MPa. When the water injection ends at around 55 s the pressure in the PC and in the VV is reduced by the ST reaching the final condition after around 300 s.

In the facility several thermal-hydraulic measurements are performed such as the pressure in the PC, VV, RP and ST, fluid temperature in the PC, SD, VV and ST, wall temperature on the PC, SD, VV and ST and boiler conditions (temperature, pressure, injected mass flow rate).

Table 1. Case4 main parameters and nominal initial conditions

Parameter	**Value**
PC, SD, VV initial wall temperature [K]	503.15
PC, SD, VV initial pressure [Pa]	1000
Injected water temperature from boiler [K]	423.15
Boiler pressure [MPa]	2
Water injection duration time [s]	45
Number of active nozzles	2
ST initial water and wall temperature [K]	293.15
MV opening PC pressure set point [MPa]	0.15

In order to study and to characterize the qualitative and quantitative TRACE code accuracy, the transient phenomenology has been divided by the authors into four main PhWs:

- PhW0 (0 – 10 s): initial phase of the transient without water injection and MV closed. The PhW ends at the beginning of the water injection.
- PhW1 (10 – 55 s): water injection in the PC with a consequent pressurization of the PC and VV due to the flashing of the injected water in the low-pressure environment and the contact with the hot surrounding walls. Soon after the beginning of the water injection, the pressure rise causes the opening of the MV activating the pressure suppression in the ST; after the opening of the MV two counteracting phenomena are present: the pressurization of the PC and VV and the pressure suppression in the ST. The variation of the weight of the two phenomena along the PhW determines the pressure evolution. The PhW ends when the water injection finishes.
- PhW2 (55 – 100 s): depressurization of the PC and VV. In this phase the water injection is over, therefore the dominant phenomenology is the depressurization due to the pressure suppression in the ST. The PhW ends when the PC and VV depressurization is completed.
- PhW3 (100 – 300 s): reaching of the final test conditions. The PC, VV and ST pressure is almost constant; the PC and VV temperature increases due to the superheating of the remaining steam by the hotter surrounding walls.

The PhWs are summarized in Table 2 together with the Relevant Thermal Hydraulic Phenomena (RTP) and the RTA occurring in each window.

Table 2: Identified PhWs, RTP and RTA

PhW	Time [s]	RTP	RTA
0	0–10	-	-
1	10–55	• Flashing of water in the PC and VV • Water condensation in the SD • Pressure suppression in the ST	• Beginning of water injection (at 10 s) • Opening of the MV • PC maximum pressure 0.465 MPa (at 23 s) • End of water injection (at 55 s)
2	55–100	• Water condensation in the SD • Pressure suppression in the ST	• Maximum pressure in the ST 0.042 MPa (at 87 s)
3	100–300	• Steam superheating in the PC and VV	• Final pressure in the PC and VV 0.051 MPa • Final pressure in the ST 0.040 MPa • Final temperature in the PC and VV 427 K

3. *TRACE code and facility nodalization description*

3.1 Description of TRACE code

TRACE (TRAC/RELAP Advanced Computational Engine) is a best-estimate thermal-hydraulic system code developed by USNRC [10]. It is a component-oriented code developed for best-estimate analysis for LWR. In particular, TRACE was designed for the simulation of operational transient, LOCAs and to model the thermal-hydraulic phenomena taking place in the experimental facilities used to study the steady-state and transient behavior of reactor fission systems [9][18]. The TRACE/SNAP environment/architecture is presented in [18][19].

The code is based on two fluids, two-phases field equations. This set of equations consists in the conservation laws of mass, momentum and energy for the liquid and gas fields [20]. In TRACE is implemented the so called “six-equations” two fluid model. The resulting equation set is coupled to additional equations for non-condensable gas, dissolved boron, control systems and reactor power. Relations for wall drag, interfacial drag, wall heat transfer, interfacial heat transfer, equation of state and static flow regime maps are used for the closure of the field equations. The interaction between the steam-liquid phases and the heat transfer from solid structures to liquid-steam is also considered. These interactions are in general dependent on flow topology and for this purpose a special flow regime dependent constitutive-equation package has been incorporated into the code. TRACE implements, pre-CHF (Critical Heat Flux), stratified and post-CHF flow regimes classes.

For vertical flow, in the pre-CHF flow regime class, bubbly/slug (used to indicate dispersed bubbles, slug flow and Taylor cap bubble regime) and annular/mist flow regimes are considered in the code. For horizontal and inclined flows, the common recognized flow regimes (stratified smooth, stratified wavy, plug/slug flow, annular/dispersed, dispersed bubble) are considered, explicitly or not explicitly in the code in the stratified regime class. The stratified smooth is explicitly considered, stratified wavy and plug/slug are treated as transition regimes (transition from stratified flow to a non-stratified flow) and annular/dispersed and dispersed bubble regimes are treated by their vertical flow analogs (annular mist and bubbly/slug). The post-CHF flow regime class comprehends the “inverted” flow regimes (inverted annular, inverted slug and disperse flow regimes) that may occur when the surface is too hot for allowing the contact between the wall and the liquid. In order to identify the different flow regimes, flow regime maps are used; they are in general function of thermal-hydraulic parameters such as superficial gas velocity, mass flux, void fraction (e.g. Post-CHF regime map is determined by superficial gas velocity and void fraction). The flow regime selected by the code is

important for the characterization of, e.g., the interfacial drag and interfacial heat transfer coefficients. A detail treatment of the two-phase flow models present in TRACE code can be found in the code theory manual [10].

In order to study the thermal history of the solid structures the heat conduction equation is applied to different geometry. A 2D (r and z) treatment of conduction heat transfer is taken into account as well. A finite volume numerical method is used to solve the partial differential equations governing the two-phase flow and heat transfer. By default, a multi-step time-differencing procedure that allows the material Courant-limit condition to be exceeded, is used to solve the fluid-dynamics equations [9][21]. In this study it has been used TRACE V5 patch 4 [10].

3.2 Description of the TRACE nodalization versus ICE facility

TRACE nodalization of the ICE facility has been developed with SNAP. The Vessel component has been used to simulate the PC, SD and VV where multidimensional phenomena could take place. TRACE's Vessel component in the default condition is a vertical cylinder with the gravitational unit vector directed in the negative z-coordinate. The user can define a different orientation of the component by setting the namelist variable NVGRAV=1 in the model specifications and then entering the gravitational unit vector components in the vessel input data [22]. This allows also to simulate horizontal cylinders such as the PC and the VV by setting the gravitational unit vector pointing in the x-coordinate.

The PC and the VV have been simulated with two Vessel components in cylindrical geometry with the gravitational unit vector pointing in the positive x-coordinate direction. The PC is divided into 18 axial levels, 4 radial rings and 12 azimuthal sectors; the VV is divided into 14 axial levels, 2 radial rings and 6 azimuthal sectors. The SD is modeled with a Vessel component in Cartesian coordinates (with the gravitational unit vector pointing in the x-coordinate as for the PC and VV) with 12 axial levels, 2 volumes in the x-direction and 1 volume in the y-direction. Each axial level is associated with one slit of the SD and the corresponding flow area and hydraulic diameter has been entered in the face specifications. Two sets of twelve Single Junctions components connects the PC to the SD and the SD to the VV. The water injecting nozzles from the boiler have been simulated by three Fill components laterally connected to the PC.

The RP is modeled with a series of Pipe components and the MV with a Valve component controlled by a trip that is the pressure set-point in the PC for the opening (0.15 MPa). The default chocking model available in TRACE code has been activated on the RP. The ST is modeled by a Pipe component with a single volume and the RP is connected to the ST through a crossflow junction. Table 3 shows the volumes of the various components of the facility and the comparison with the experimental data.

Heat Structures have been added to simulate the solid structures of the facility: PC, VV and ST walls, RP pipe wall, flanges and insulation. A convective heat transfer coefficient and the ambient temperature have been set on the outer surface of heat structures to simulate heat losses from the facility. A scheme of the facility nodalization, made with SNAP, is shown in Fig. 2.

Table 3 Volumes of the components in the facility versus TRACE nodalization

Component	Facility [m^3]	TRACE [m^3]	Relative error [%]
PC	0.60	0.594	1.0
SD	0.02	0.020	0.0
VV	0.34	0.338	0.6
RP	0.01	0.010	0.0
ST	0.93	0.930	0.0

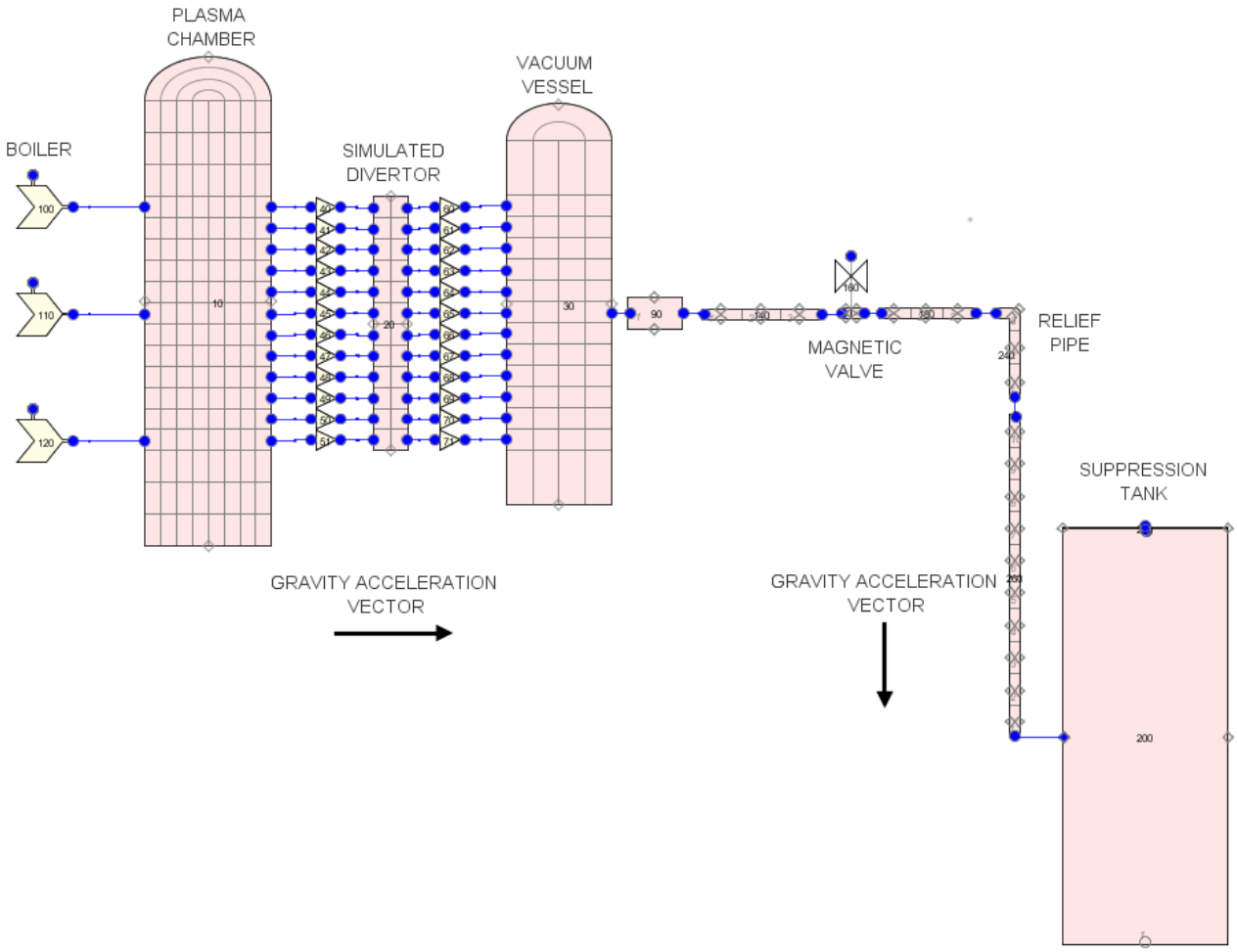

Fig. 2. TRACE nodalization of ICE facility made with SNAP

4. *Results of reference calculation*

The calculated PC, VV and ST pressure and the PC and VV temperature are compared to the experimental results in Fig. 3 to Fig. 7, with the four PhWs previously identified marked by dashed lines. After reaching the Start Of the Transient (SOT) conditions specific of the test, the transient has been simulated by TRACE code. Table 4 shows the comparison of the initial conditions obtained by the TRACE code against the experimental initial conditions.

Table 4 Comparison of experimental and calculated initial conditions

Parameter	**Experimental data**	**Calculated data**	**Relative error [%]**
PC pressure [Pa]	1000	1000	0.00
VV pressure [Pa]	1000	1000	0.00
ST pressure [Pa]	4000	4048	1.20
PC temperature [K]	503.45	503.15	0.06
VV temperature [K]	503.75	503.15	0.12
ST temperature [K]	294.75	293.15	0.54

The relative error has been computed as the absolute value of the difference between the calculated and the experimental data divided by the experimental data. In order to set the initial condition for the ST, the component has been assumed by the authors in thermal equilibrium with the ambient, also because it is not insulated. The ST gas initial pressure is the sum of the steam saturation pressure and air partial pressure in order to get the experimental initial condition.

In PhW0 the considered parameters are almost constant since no relevant actions or phenomena occur.

As in the experimental data available, the water injection in the PC starts at 10 s, determining the beginning of PhW1. Due to the flashing of the pressurized water in the PC low-pressure environment and the contact with the hot surrounding walls, a strong pressure increment takes place in the PC (Fig. 3) and in the connected VV (Fig. 4). Before the opening of the MV the only phenomenon which occurs is the PC and VV pressurization.

When the pressure in the PC reaches 0.15 MPa, there is the opening of the MV, with the inception of water discharging in the ST that causes the ST pressure rise (Fig. 5). After the opening of the MV the pressure suppression in the ST begins, therefore in the remaining part of PhW1 two counteracting phenomena are present: the pressurization of the PC and VV and the pressure suppression in the ST. The variation of the weight of the two phenomena along the PhW determines the pressure evolution. In fact, initially the pressure suppression in the ST has a low phenomenological weight and the PC and VV pressure continue to increase. Then, in the experimental data, a change of slope in the PC and VV is observed (at around 13.5 s), showing the increase of weight of the depressurization phenomenology and a pressure maximum is reached in the PC (at around 23 s) and in the VV (at around 23.5 s).

Initially, the pressure rise is qualitatively and quantitatively predicted by the code. After around 13 s, the PC and VV pressure increase predicted by the code is slightly lower than the experimental one. A first PC pressure peak is reached by TRACE code at about 25 s with a pressure value of 0.457 MPa. A delay of about 2 s is observed in comparison with the experimental data.

In the PC and in the VV, the entrance of colder pressurized water (in comparison to the initial wall temperature shown in Table 1) and the steam expansion leads to a sudden drop of the temperatures in the PC and VV atmosphere (Fig. 6 and Fig. 7). The temperature drop in the atmosphere of the PC is qualitatively predicted even if with a bigger decrease in comparison with the experimental data. After the initial decrease, the PC temperature rises, reaching a plateau corresponding to the saturation temperature (at around 420 K) and the behavior is predicted by the calculated data. In relation to the VV atmosphere temperature, the code predicts initially a bigger decrease in comparison with the experimental data and a subsequent increase and decrease before reaching the plateau as in the experimental results.

After the reaching of the maximum value, the experimental PC and VV pressure slightly reduce in the second part of PhW1. In this phase, both the pressurization of the PC and VV and the pressure suppression in the ST take place. However, in this phase, the latter has a major phenomenological weight and, as a consequence, the PC and VV pressure slightly decrease in the experimental data. The PC and VV pressure behavior is predicted by the code in this phase, even if the calculated results show a small pressure peak at the end of the PhW (with an initial pressure decrease and a further pressure increase reaching 0.464 MPa), not observed in the experimental results.

The MV is fully open and the ST experimental pressure continue to increase with an almost constant rate. The ST pressure increase is qualitatively and quantitatively predicted by the calculation, Fig. 6.

The temperature in the PC and in the VV is at saturation (around 420 K) and it remains almost constant. The calculation predicts the condensation of steam in the SD as visually observed in the experiment [5]. Since the observation of the phenomena is only visual, and there is no instrumentation to measure it, the comparison with the calculation can be only qualitative and not quantitative.

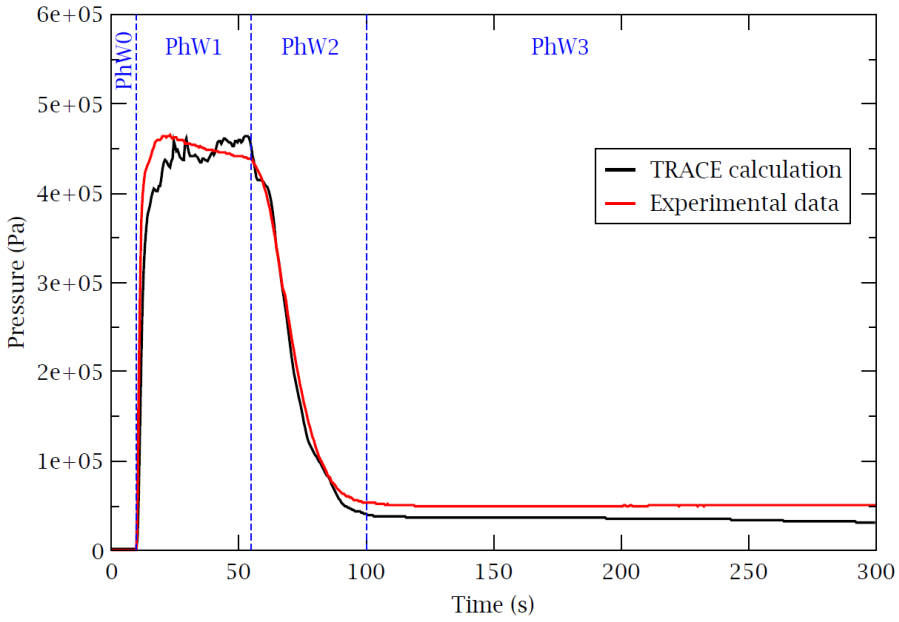

Fig. 3 PC pressure behavior vs time

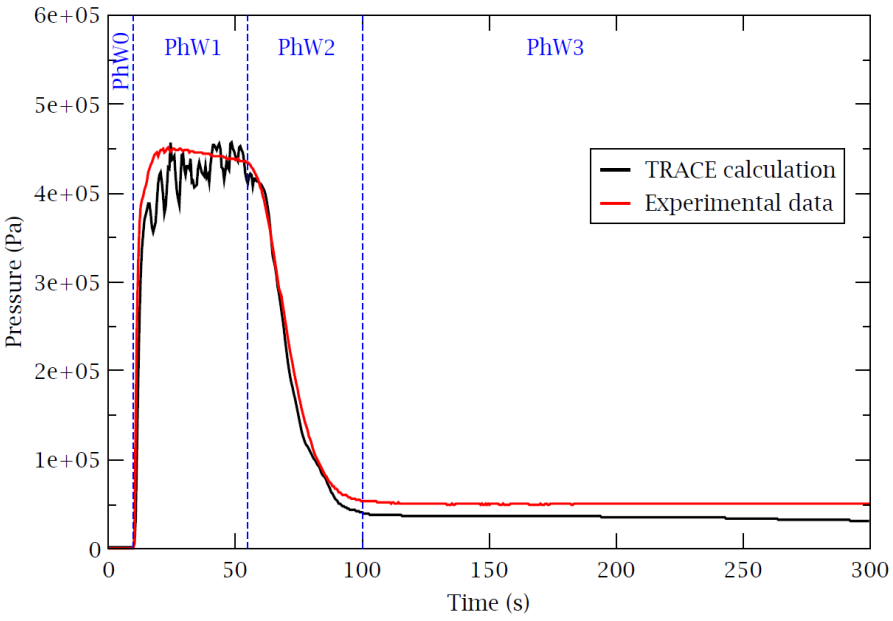

Fig. 4 VV pressure behavior vs time

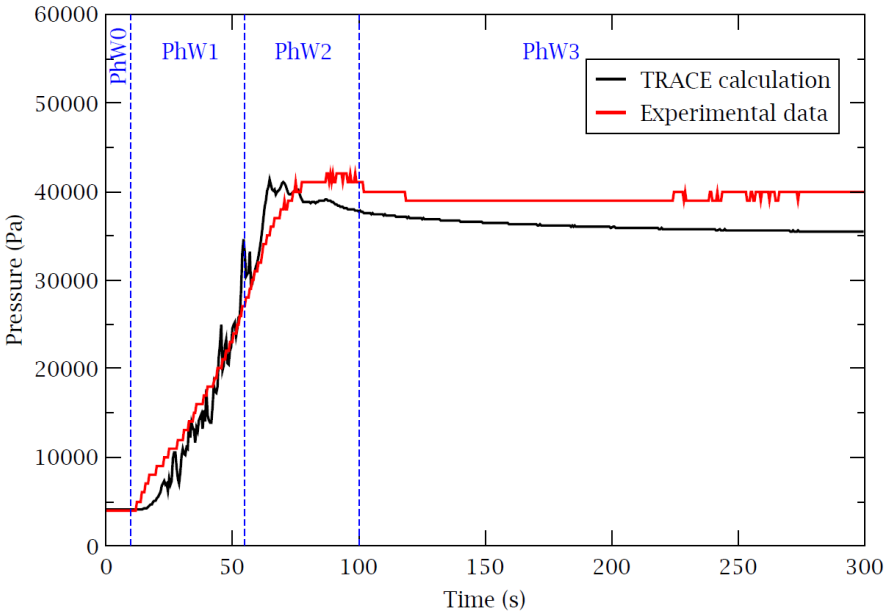

Fig. 5 ST pressure behavior vs time

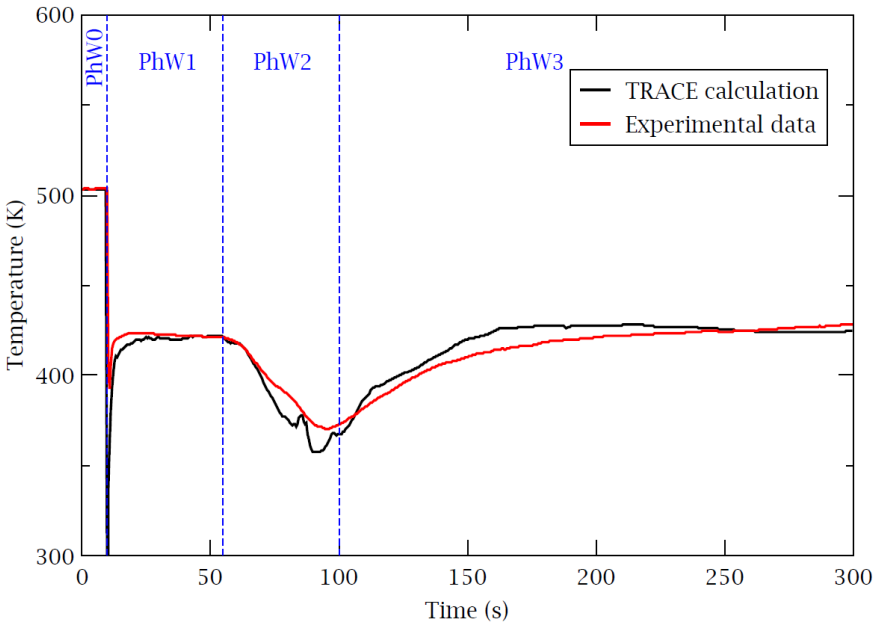

Fig. 6 PC temperature behavior vs time

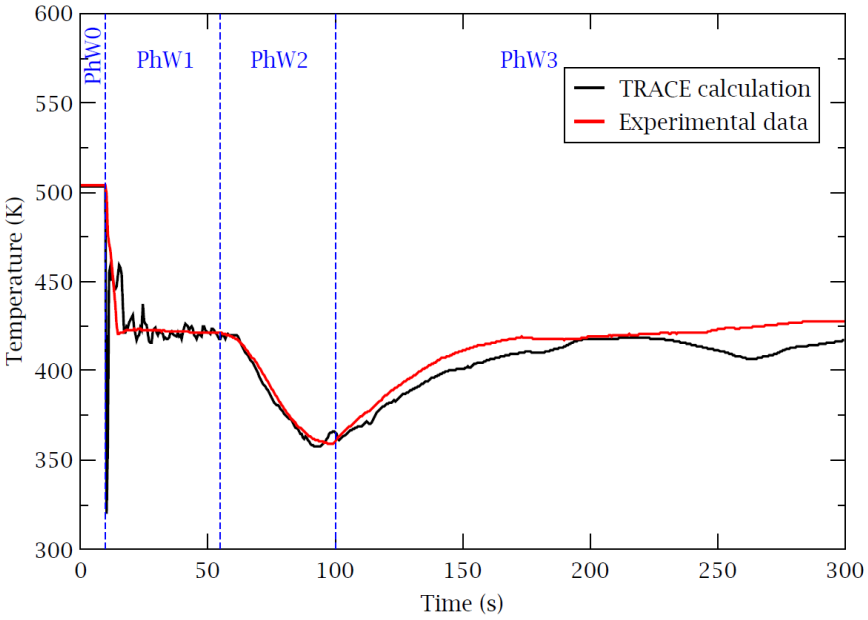

Fig. 7 VV temperature behavior vs time

PhW2 begins at the end of the water injection in the PC (at 55 s); the pressure in the PC and in the VV drops, since water is continuously discharged in the ST, reaching a value around 0.05 MPa after about 100 s. The ST pressure continues to rise and then stabilizes at 0.04 MPa after around 90 s. In this phase, the temperature in the PC and VV initially decreases following the saturation one until the end of the depressurization and then it rises again for the superheating of the steam remaining in the PC and VV. Therefore, it is possible to identify PhW2 from 55 s to 100 s consisting in the depressurization of the PC and VV and in the final pressurization of the ST. In this PhW, all the parameters are qualitatively and quantitatively correctly predicted by the calculation. The PC and VV depressurization, and the consequent temperature decrease, is correctly simulated, with a slight underestimation of the PC and VV pressure at the end of the PhW. The final part of the ST pressurization is correctly predicted, even if the ST maximum pressure is slightly anticipated in the calculation.

The final part of the transient consists in the reaching of the final conditions of the test and this is the last PhW from 100 s to 300 s. The pressure in the PC and VV is almost constant around 0.05 MPa. Also the ST pressure is almost constant in this PhW and close to 0.04 MPa. The temperature in the PC and VV, after the depressurization phase, rises due to the superheating of the remaining steam and stabilizes around 425 K. The PC and VV calculated pressure is constant and slightly lower than the experimental one. This could be due to the heat structures in the model; in fact, some discrepancies with respect to the experimental facility may be present e.g. for the flanges, the ports for the instrumentation and the visual observation, for the structural supports, for auxiliary piping, etc. As a future activity it could be considered a more detailed analysis of heat structure to improve the code prediction in PhW3.

The ST pressure has a little decrease at the beginning of the PhW, as in the experimental results, and then it is almost constant in the final part of the PhW, showing an underestimation of the final pressure. The calculated PC and VV temperature qualitatively and quantitatively agree with the experimental results and the steam superheating is correctly predicted.

In Table 5, the experimental RTPs and RTAs occurring in each PhW are compared with the TRACE prediction. All the phenomena are qualitatively predicted by the code in the correct PhW, some slight differences are present in the timing and in the values of the computed RTAs.

Table 5: Comparison of the experimental and calculated RTPs and RTAs

PhW	Time [s]	EXP_RTP	EXP_RTA	TRACE_RTP	TRACE_RTA
0	0–10	-	-	-	-
1	10–55	• Flashing of water in the PC and VV • Water condensation in the SD • Pressure suppression in the ST	• Beginning of water injection (at 10 s) • Opening of the MV • PC maximum pressure 0.465 MPa (at 23 s) • End of water injection (at 55 s)	• Flashing of water in the PC and VV • Water condensation in the SD • Pressure suppression in the ST	• Beginning of water injection (at 10 s) • Opening of the MV (at around 12 s) • PC maximum pressure 0.464 MPa (at 53 s) • End of water injection (at 55 s)
2	55–100	• Water condensation in the SD • Pressure suppression in the ST	• Maximum pressure in the ST 0.042 MPa (at 87 s)	• Water condensation in the SD • Pressure suppression in the ST	• Maximum pressure in the ST 0.041 MPa (at 76 s)
3	100–300	• Steam superheating in the PC and VV	• Final pressure in the PC and VV 0.051 MPa • Final pressure in the ST 0.040 MPa • Final temperature in the PC and VV 427 K	• Steam superheating in the PC and VV	• Final pressure in the PC and VV 0.035 MPa • Final pressure in the ST 0.036 MPa • Final temperature in the PC and VV 429 K

5. Qualitative and quantitative accuracy evaluation

The results obtained with computer codes should undergo a rigorous process of accuracy evaluation to assess their quality. Accuracy is defined as the discrepancy between the calculated results and the experimental ones and accuracy evaluation is part of the Code Independent Qualification process [12] performed by the code users.

The accuracy evaluation is performed in two steps:

1) Qualitative accuracy evaluation;
2) Quantitative accuracy evaluation.

The qualitative evaluation is a subjective judgment of the calculated results by the code-user while the quantitative evaluation is a procedure that can give a numerical indication of the performance of a calculation.

5.1 Qualitative accuracy evaluation

The qualitative accuracy evaluation begins with the identification of the PhWs of the transient and the RTPs in each window, which have been previously described. Then the RTA that characterize the RTPs are identified. The qualitative evaluation is performed with a visual comparison of the calculated and experimental results giving a subjective judgment to each RTP previously identified.

In the present study, the qualitative analysis is based on four subjective judgment marks (Excellent (+), Reasonable (o), Minimal (NA), Unqualified (-)), that are given both to the experimental data and to the calculated ones. Table 6 shows the meaning of the experimental and calculated data qualitative accuracy evaluation.

For the analyzed transient three main phenomena have been identified and it has been evaluated the availability of experimental measurements to characterize them, as reported in Table 7.

Table 6. Judgement marks for the qualitative accuracy evaluation [9]

	+	o	NA	-
Experimental data	Phenomenon occurred in the test and it is directly measured	Phenomenon occurred in the test and it is indirectly measured	Phenomenon occurred during the test but there is no instrumentation to detect (lack of instrumentation)	Phenomenon not occurred in the test
Calculated data	Phenomenon is clearly predicted by the code (**Excellent**)	Phenomenon is partially predicted (i.e. the answer of the code is **reasonable** but closure code relations are not appropriate, etc.)	Models are not appropriate to predict (i.e. nodalization strategy, etc.) (**Minimal**)	Phenomenon is not predicted by the code (**Unqualified**)

Table 7. Qualitative evaluation of the phenomena in the integrated ICE facility and capability of the code to reproduce them

	Phenomenon	**Experiment**		**Code**
		Phenomena	**Measurement**	**Phenomena**
A	Flashing of water in the PC and VV	+	• PC pressure • VV pressure • PC temperature • VV temperature	+
B	Condensation in the SD	o/NA*	Only visual observation, not experimentally quantified	+
C	Pressure suppression by the ST	+	• PC pressure • VV pressure • ST pressure	+

* The phenomenon occurs in the facility; it is visually detected, but it is not directly or indirectly measured.

The pressurization of the PC and VV due to the flashing of water and the depressurization due to the operation of the ST, acting as a pressure suppression system, can be characterized by the available experimental measurement. The steam condensation in the SD has been observed visually [5]. Considering the results of the code and the qualitative evaluation, reported in Table 7, it is possible to conclude that the code is qualitatively able to predict all the phenomena and the behavior of the parameters selected in the analysis.

5.2 Quantitative accuracy evaluation

The quantitative evaluation of the code results has been carried out using the FFTBM to asses in a quantitative way the accuracy of a code calculation against available experimental data. In this method, the difference between the calculated data and the experimental one is passed from the time domain to the frequency domain using the Fast Fourier Transform. Then, the accuracy evaluation is performed on two parameters: the Average Amplitude (AA) and the Weighted Frequency (WF) [23][24]. The AA is used as an indication of the code accuracy; the lower is the AA, the more accurate is the result. The WF gives information about the frequencies that more significantly contribute to the discrepancies between the calculated and the experimental data. The accuracy evaluation is mainly based on the AA parameter, while the WF is an additional qualitative information that may be considered for the accuracy evaluation [13].

Usually several parameters are selected for the accuracy evaluation, and for each parameter the AA and the WF are calculated. Therefore, from the AA and the WF of each parameter, the total weighted average amplitude and the total weighted frequency are computed using proper weighting factors. In the original methodology, the weighting factors consider the experimental accuracy, the safety relevance and the parameter contribution to the primary pressure (since the method was initially developed for LOCAs in PWR). In this study the weighting factors have been set equal to one for all parameters, so they all have the same importance. The FFTBM has been applied in a default way but, as previously underlined, not considering the weighting factors. The tool adopted to perform the FFTBM analysis is the JSI FFTBM Add-In 2007 developed at Jožef Stefan Institute (Slovenia) [23][24][25].

The FFTBM has been performed and the AA and the WF have been computed for the five selected parameters in the four PhWs previously identified. The reference threshold values for the AA for the accuracy evaluation are [26]:

- $AA_{tot} \leq 0.3$: very good code prediction;
- $0.3 < AA_{tot} \leq 0.5$: good code prediction;
- $0.5 < AA_{tot} \leq 0.7$: poor code prediction;
- $AA_{tot} \geq 0.7$: very poor code prediction.

The results of the quantitative accuracy evaluation are shown in Table 8.

Table 8 Results of the quantitative accuracy evaluation with FFTBM

	PhW0		**PhW1**		**PhW2**		**PhW3**	
Parameters	**AA**	**WF**	**AA**	**WF**	**AA**	**WF**	**AA**	**WF**
PC pressure	0.00	0.22	0.25	0.11	0.07	0.10	0.47	0.03
VV pressure	0.00	0.22	0.23	0.13	0.07	0.07	0.46	0.03
ST pressure	0.01	0.01	0.28	0.15	0.18	0.10	0.18	0.05
PC temperature	0.09	0.22	0.19	0.17	0.06	0.07	0.04	0.03
VV temperature	0.00	0.03	0.23	0.19	0.03	0.09	0.06	0.06
Total	0.02	0.14	0.24	0.15	0.08	0.09	0.24	0.04

Analyzing the FFTBM results, it is possible to notice that the total AA in each PhW is lower than 0.3 (which is the threshold between a good and a very good prediction). Therefore, the prediction is always very good according to the previous classification.

Looking more in detail at each parameter, the AA is lower than 0.3 for almost all parameters in each PhW. Only in PhW3 the AA is close to 0.5 for the PC and VV pressure due to a slight underestimation of the experimental pressure. In general, considering both the AA for each parameter and the total AA in all the PhWs, the quantitative accuracy results can be classified as very good.

6. Uncertainty Analysis

6.1 Description of the UA method

Best-estimate thermal-hydraulic computer codes have reached a high level of maturity in the last decades, however in their application some sources of uncertainty are still present and affect code results [12]. In general, the sources of uncertainty can be divided into [27]:

- Code uncertainty (e.g. approximation in the conservative equation and in the closure models and correlations);
- Representation uncertainty (nodalization effect);
- Scaling (the codes are in general validated against scaled down facilities);
- Plant uncertainty (e.g. initial and boundary conditions);
- User effect.

For these reasons, the execution of an UA has a great importance in the evaluation of results obtained with computer codes. Several methodologies have been developed in the past to perform UA. In particular these uncertainty methodologies can be grouped in [27]:

a) Methods to propagate input uncertainty, divided in:
   - Probabilistic (e.g. CSAU, GRS, IPSN, etc.);
   - Deterministic (e.g. AEAW, EDF-Framatome, etc.);
b) Method to extrapolate output uncertainty (e.g. UMAE).

Among these methodologies the probabilistic propagation of input uncertainties [14] is particularly suitable to be coupled with computer codes since it is based on the creation of a number of code runs with different input uncertain parameters to characterize the uncertainty of the output FOM, target of the analysis. In this method the uncertain input parameters are sampled in a random way to create a set of code inputs; the inputs are run independently and then response correlations are applied to characterize the relationship between the input uncertain parameters and the output, in terms of selected FOMs. The input parameters are defined by their reference value, range of variation and Probability Density Function (PDF) type [28]. Several uncertainty tools have been developed based on this methodology. In this application DAKOTA [15], developed by Sandia National Laboratories, has been used.

6.2 Description of DAKOTA tool in SNAP environment/architecture

DAKOTA [15] is developed by Sandia National Laboratories to perform parametric and uncertainty analysis in a fast and automatic way. The aim of this toolkit is to bridge simulation codes and analysis method for parametric evaluation, uncertainty qualification and system optimization [29]. DAKOTA toolkit is also provided as a plug-in [30] for SNAP, which is described afterwards.

In particular, DAKOTA plugin for SNAP allows to:

1) Enter the selected uncertain input parameters (together with their range and PDF type);

2) Select the sampling method (Monte Carlo or Latin Hypercube);
3) Enter the desired FOMs for the analysis;
4) Set the final report, automatically generated at the end of the uncertainty quantification analysis, which contains the results of the uncertainty analysis application.

In Fig. 8 it is presented the DAKOTA workflow in SNAP coupled with TRACE code. Starting from the reference TRACE input, the selected uncertain input parameters (together with their range and PDF) and the FOMs, DAKOTA samples the input parameters creating a set of N TRACE inputs. The minimum number of code runs N depends on the requested probability content α, the confidence level β and the number of FOMs. In case only one FOM is investigated, for the one-sided tolerance interval, the required number of code runs can be found, based on Wilks [31][32], by solving the following equation with respect to N:

$$1 - \alpha^N = \beta \tag{1}$$

If more than one FOM is investigated, for the one-sided tolerance interval, the required number of code runs can be found by solving the following equation with respect to N [33]:

$$\beta = \sum_{j=0}^{N-p} \frac{N!}{(N-j)!\,j!} \alpha^j (1-\alpha)^{N-j} \tag{2}$$

where p is the number of FOMs. More information on statistical aspects of best estimate analyses can be found in [34].

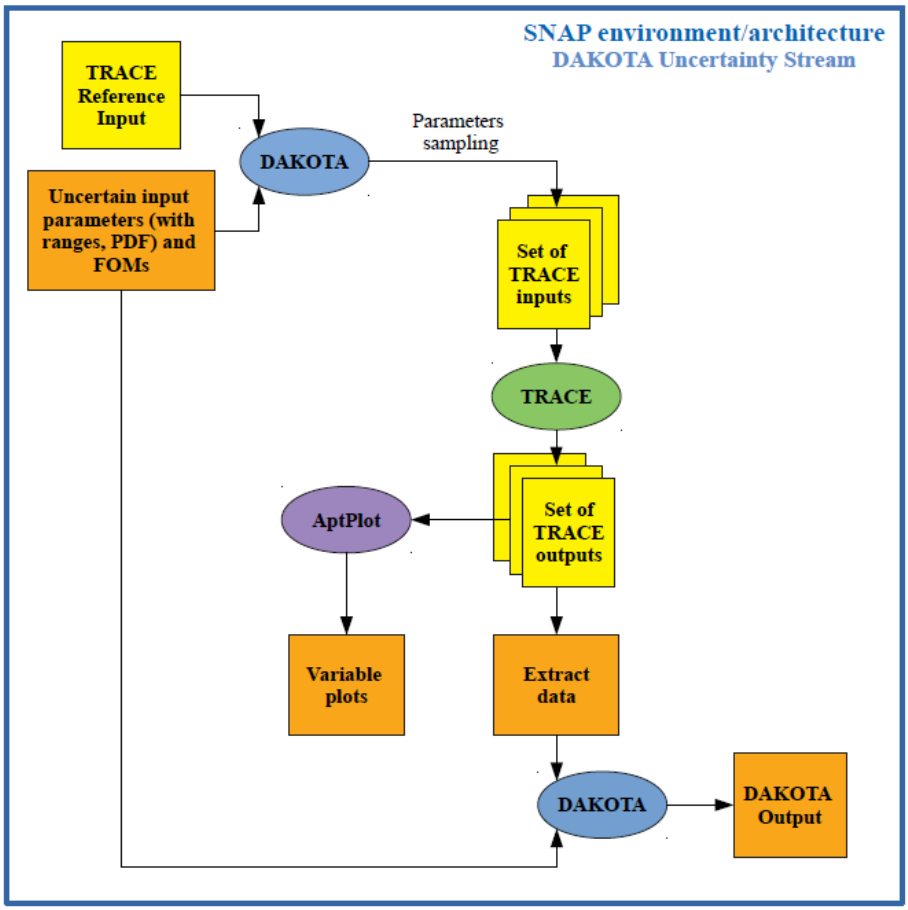

Fig. 8 DAKOTA workflow in the SNAP environment/architecture [28]

The set of N TRACE inputs is solved and a set of N TRACE outputs is created. Then through AptPlot [35] it is possible to plot the time dependent behavior of the desired variables. Using DAKOTA it is possible to perform the statistical analysis and to characterize, through response correlations, the relationship between the selected uncertain input parameters and the FOMs. This can be performed adding an Extract Data step to the DAKOTA Uncertainty Stream.

As a result of the uncertainty analysis, DAKOTA [15][30][36] computes four response correlation coefficients: simple, partial, simple rank and partial rank. The simple coefficients are related to the actual input and output data. The simple coefficient r between an input variable x and an output variable y, in n samples, is computed using the Pearson's correlation. It is a measure of the degree of linear correlation between the two variables and its value is comprised between -1 and 1. If $r<0$ the correlation is negative (an increment of x leads to a reduction in y), if $r=0$ there is no correlation between the two variables, if $r>0$ the correlation is positive (an increment of x leads to an increment of y).

The partial correlation coefficient is computed similarly to simple ones but taking into accounts the effects of the other variables. Rank correlations uses the ranked data instead of the actual ones. Ranks are obtained by ordering the data in ascending order, and they are more convenient to be used when inputs and outputs are characterized by sensible difference in magnitude; it is possible to understand if the input sample with the lower rank is associated to the output with the lower rank and so on [15][36]. To compute the rank correlation in DAKOTA it is used the Spearman's rank correlation that is similar to Pearson's one but using the ranked data instead of the actual values. If two variables are monotonically related, without repetitions, the Spearman coefficient is -1 or +1 (depending if the function is monotonically decreasing or increasing), since the ranked values are used. Moreover, Spearman's correlation is less sensitive to possible outlier values of the variables than Pearson's one.

6.3 Hypothesis adopted in the UA

The selection of the parameters for the UA depends on the available data concerning the geometry of the facility and its component, the initial and boundary conditions of the experiments and on the control logic. Once the parameters have been selected, for each of them it should be identified:

1) The reference value;
2) The range of variation of the parameter;
3) The associated PDF.

The definition of the PDF is one of the most challenging task in the application of the probabilistic method to propagate input uncertainties. If there is no evidence or information to choose a particular PDF, the uniform distribution can be used; in fact, at a fixed range, it assigns the same probability to all the values in the range of variation of the parameter. The drawback is that this can lead to a results spreading larger than the one obtained with the use of peaked type distributions. More information about deriving parameter PDF can be found in [37].

In Table 9 the selected uncertain input parameters are listed with their range and PDF. The PDF type and the range of variation for some parameters (marked with an * in Table 9) have been derived from an analysis of ingress of coolant event performed with RELAP5 code and SUSA tool for the Wendelstein 7-X (W7-X) stellarator in Germany **Errore. L'origine riferimento non è stata trovata.**. For the remaining input parameters without specific information, engineering judgement has been adopted for the reference value with a large range [-100%; +100%] and the uniform distribution in order to have a conservative estimation.

Nine uncertain parameters with eight distributions have been considered; in fact, since the ST has been assumed in thermal equilibrium with the ambient the SOT, the ST initial temperature and external temperature have the same distribution and are sampled together.

The PC pressure has been selected as FOM since it is the most relevant safety parameter for the current analyses. With one FOM and with a probability content of 95% and a confidence level of 95%, a total of 59 calculations were required, based on Wilks, for the one-sided tolerance interval [14].

Table 9. Uncertain parameters selected for the analysis

Parameter	Range of variation	PDF type
ST initial temperature and external temperature*	[-5%; +5%]	Uniform
Boiler temperature*	[-3%; +3%]	Normal
Boiler pressure*	[-3%; +3%]	Normal
PC, SD, VV initial pressure*	[-20%; +20%]	Normal
PC, SD, VV initial temperature*	[-3%; +3%]	Uniform
Minor loss coefficient at the SD slits	[-100%; +100%]	Uniform
Minor loss coefficient at the MV	[-100%; +100%]	Uniform
MV opening delay	[-100%; +100%]	Uniform

6.4 Results of Uncertainty Analysis

All the 59 runs needed, based on the requested probability content and confidence level, have been completed successfully. The present study is focused on the characterization of the results dispersion against the experimental data and of the relationship between the selected uncertain input parameters and the FOM, through response correlations. Therefore, the time dependent behavior of the PC, VV and ST pressure and PC and VV temperature has been plotted for all 59 cases and compared to the experimental results to observe if the experimental data lies in the simulation results dispersion band. Response correlations have been applied to the FOM of the analysis (the PC pressure) to characterize the correlation between the selected uncertain input parameters and the selected output.

6.4.1 Dispersion of the results

In order to characterize the dispersion of the results the following parameters have been considered: the PC and VV pressure (Fig. 9 and Fig. 10 respectively), the ST pressure (Fig. 11) and the PC and VV temperature (Fig. 12 and Fig. 13 respectively), as it has been done for the reference calculation.

In PhW0, the dispersion of the calculated results is only related to the choice of the uncertain input parameters (initial ST temperature, and initial PC/VV pressure and temperature) and, considering Table 9, the experimental data is within the calculated results.

In PhW 1 (10 – 55 s) initial phase (10 – 15 s), the initial pressure increment in both the PC and VV has a negligible result dispersion band, while it begins to spread at around 0.25 MPa, with a band width around 0.15 MPa. In the second part of PhW1 (15 – 55 s), the dispersion band width is larger than in the previous phase around 1.7 MPa, with an average value of around 0.45 MPa. The experimental PC and VV pressure are always comprised between the calculated results. In relation to the PC, the majority of the calculations reach the maximum pressure before the end of PhW1 but with some delay in comparison with the experimental data. In these calculations, though with some delay, the decrease of pressure is predicted before the end of the water injection. The pressure peak has a dispersion of around 2.0 MPa.

In relation to the ST, the dominant phenomenology is its pressurization in both experiment and calculated data, and the experimental results is within the calculated results dispersion band. The

dispersion band width increases along the PhW, reaching a maximum value of about 0.03 MPa at the end of PhW1.

In relation to the PC atmosphere temperature, the first temperature decrease and consequent increase is simulated by all the TRACE calculation that show a higher temperature decrease in comparison with the experimental data, with a dispersion of around 100 K. While the experimental data shows a temperature plateau, some calculation show a temperature increase with a consequent temperature decrease and then, in agreement with the experimental data, the plateau. The width of the dispersion band slightly reduces, with respect to the negative peak, in the temperature increase phase (around 80 K) and then it furtherly reduces when the plateau is reached (around 25 K). Similar considerations can be drawn for the VV temperature. The VV experimental temperature show a lower temperature reduction peak, and in general the experimental data are not bounded by the calculated data only between 11 s and 13 s.

In PhW2 (55 – 100 s), when the depressurization of the system occurs, the PC and VV experimental pressure is bounded by the calculated results. All the calculations correctly predict the depressurization in this phase. The pressure dispersion band width is around 0.15 MPa, while the time dispersion band of the PC and VV pressure decrease is around 15 s.

The ST experimental pressure continues to increase and it reaches a maximum at the end of the PhW. Also the ST experimental pressure is within the calculated results, even if all the calculations anticipate the pressure peak, as observed in the reference calculation. The dispersion band width is around 0.03 with an average value around 0.04 MPa.

In this PhW, the PC and VV temperature decreases following the saturation temperature correspondent to the pressure present in the PC and VV. The experimental result is comprised within the calculated one; the dispersion band width is around 35 K and the time dispersion band of the temperature decrease is a bit lower than 20 s, consistently with the results found for the PC and VV pressure decrement.

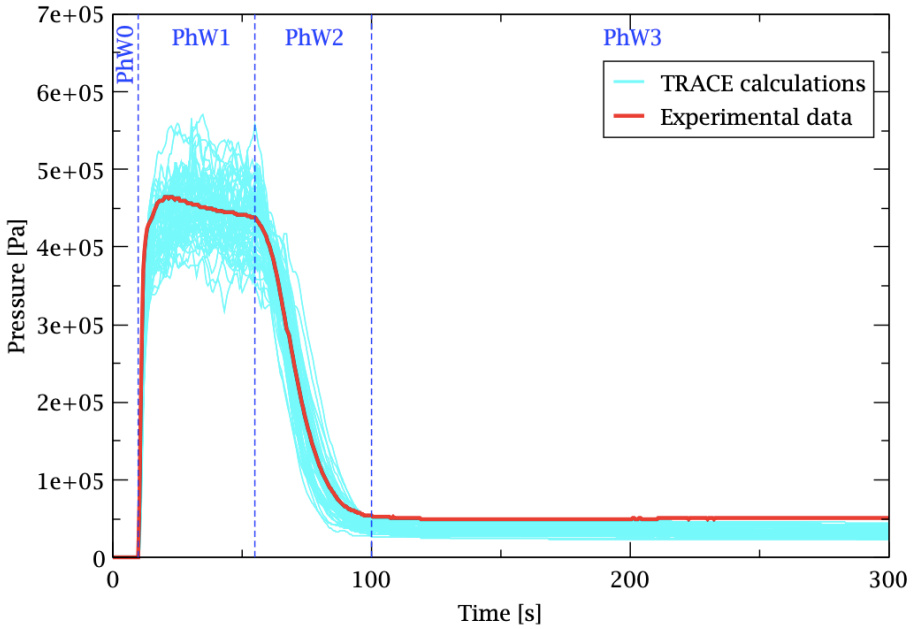

Fig. 9 Dispersion of the calculated data of the PC pressure vs experimental data

In the final PhW (100 – 300 s) the PC and VV pressure is constant and the calculated results slightly underestimate the experimental value, as observed in the reference calculation. The fact that all the calculated data are lower than the experimental value may confirm that a slight discrepancy could be present in the PC and VV heat structures, as mentioned in the discussion of the reference

calculation results. The pressure dispersion band width reduces in PhW3 (around 0.02 MPa) but it remains noticeable if compared to the average value (around 0.04 MPa).

Considering the ST pressure, the experimental data is within the calculated results. The dispersion band width is relatively wide, and its value is around 0.03 MPa with an average ST pressure value around 0.035 MPa.

In this last PhW, the fluid remained in the PC and VV is superheated by the solid structures having a higher temperature. Both the PC and VV temperature experimental data are inside the result dispersion band in the entire PhW. Starting from the minimum of the PC temperature at around 100 s the dispersion band width enlarges up to around 55 K with a final PC average temperature value of around 425 K. The VV temperature has a similar behavior but with a slightly lower dispersion band (around 45 K) and average final value (around 415 K).

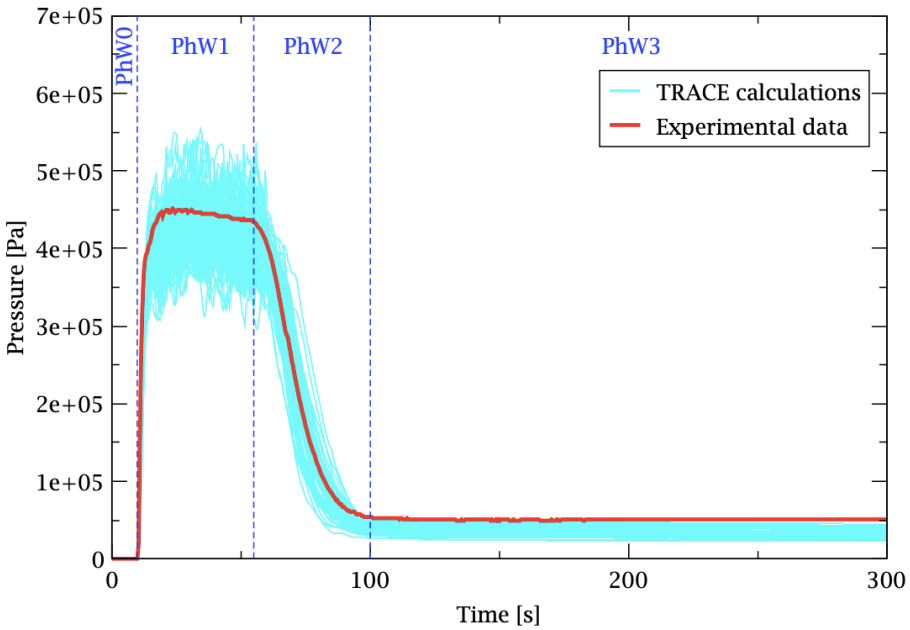

Fig. 10 Dispersion of the calculated data of the VV pressure vs experimental data

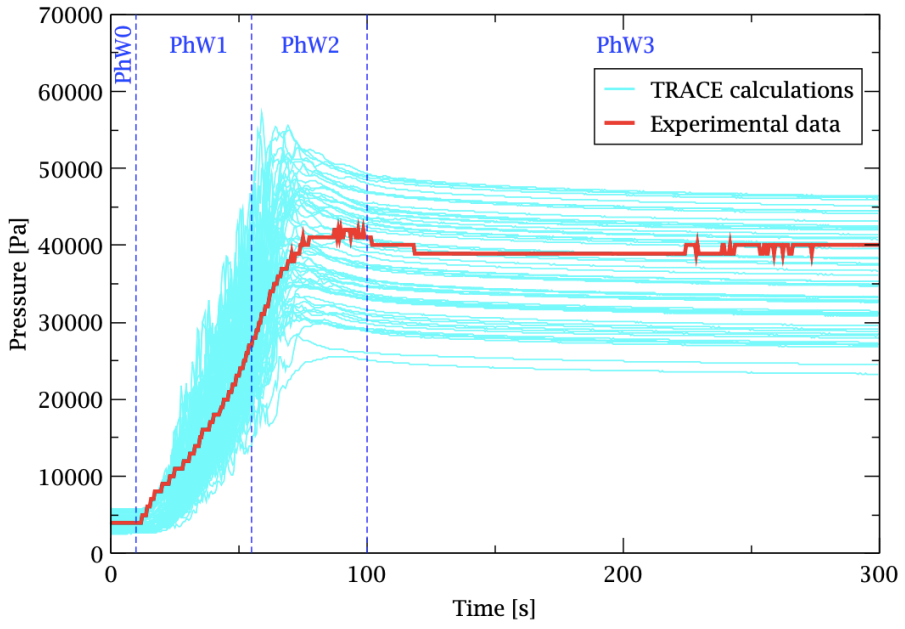

Fig. 11 Dispersion of the calculated data of the ST pressure vs experimental data

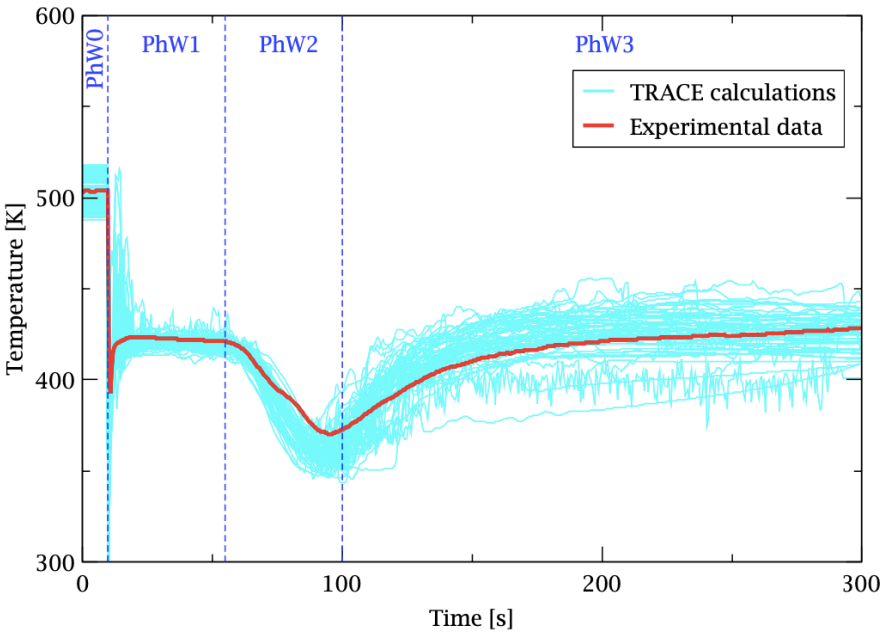

Fig. 12 Dispersion of the calculated data of the PC temperature vs experimental data

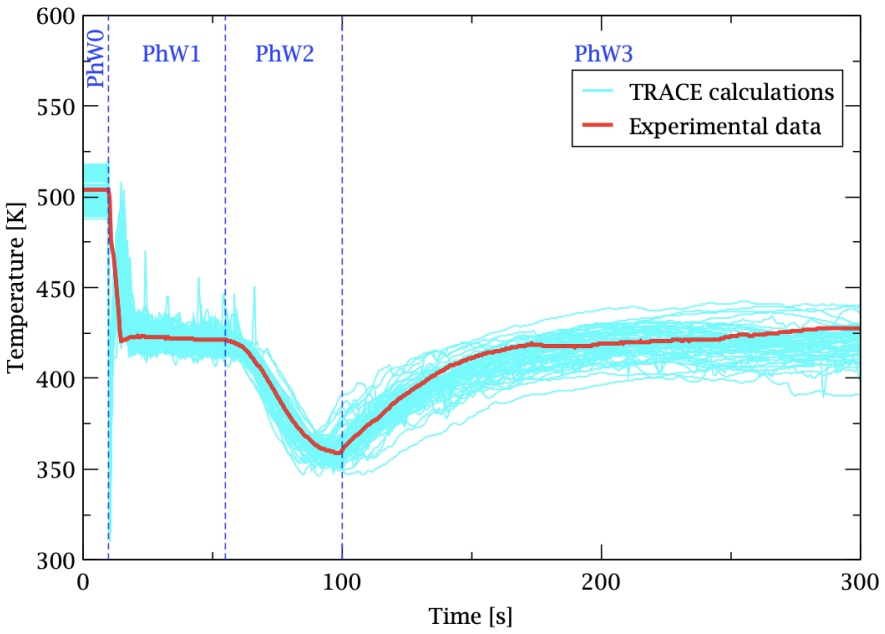

Fig. 13 Dispersion of the calculated data of the VV temperature vs experimental data

6.4.2 Response correlations results

As a result of the UA, response correlations are computed for the eight distributions, since the beginning of water injection, to measure the relationship between the selected uncertain input parameters and the chosen FOM. The two response correlations coefficient calculated provide different information: the Pearson correlation coefficient, which is an indication of the linear relationship between the input and the output, is reported in Fig. 14; the Spearman's rank correlation coefficient, which is an indication of the monotonic relationship between the input and the output, is reported in Fig. 15. The time dependent analysis of these two coefficients for the different selected uncertain input parameters is performed extracting the FOM value at selected time instants during the

transient. This allows to understand if the relationship between the selected uncertain input parameters and the chosen FOM varies during the transient in the different PhWs considered.

On both graphs the values 0.2 and 0.5 (and -0.2 and -0.5) have been highlighted as measure of the correlation between the input parameter and the FOM. As indicated in [36], for the Spearman coefficient, if the coefficient is higher than 0.5 (or lower than -0.5) the correlation is significant, if it is between 0.2 and 0.5 (or -0.2 and -0.5) the correlation is moderate, otherwise it is low. In this application, the two response correlations show similar trends; the main advantage of this time dependent analysis is the possibility to characterize the correlation of the different selected input parameters on the uncertainty of the chosen FOM in all the phases of the transient.

In PhW1 (10 – 55 s), at the beginning of the water injection, the PC initial pressure has a significant correlation (around 0.95) with the FOM, which is the PC pressure itself, as expected. The boiler temperature has the Pearson and Spearman coefficients between 0.62 and 0.87 since higher is the water temperature higher is the flashing due to the higher difference with respect to the saturation temperature in the PC. Therefore, the correlation with the FOM is significant and almost linear. In PhW1, when the opening of the MV occurs, also the MV opening delay has a moderate correlation with the PC pressure (between 0.20 and 0.37). In fact, larger is the valve opening delay, later the ST is activated and higher is the PC pressure.

The minor loss coefficient at the SD slits has a positive moderate correlation to the PC pressure (between 0.20 and 0.33) since, with a higher pressure drop in the SD, the pressure in the PC remains higher. Also the minor loss coefficient in the MV have a moderate correlation to the FOM, up to 0.40. In fact, the ST is active and with a higher pressure drop in the MV the pressure in the VV and consequently in the PC remains higher. Finally, the PC initial temperature has a moderate correlation with the FOM (up to 0.29) since with a higher initial temperature of the PC, when the injected water touches the hot walls more heat is transferred to the fluid and the pressurization is higher. All the other input uncertain parameters have a low correlation to the PC pressure in this PhW.

In PhW2 (55 – 100 s) the relationship between the minor loss coefficient in the MV and the PC pressure rises and becomes significant positive, with a maximum value around 0.66 both for the Pearson and Spearman coefficients. This is the depressurization phase of the transient and the pressure in the PC and VV is significantly correlated to the pressure drop in the pressure relief line and so in the MV. In this PhW, the boiler temperature correlation to the PC pressure turns to be moderate negative, with a minimum value around -0.35. This is due to the fact that with a lower injection temperature the PC pressure remains lower in PhW1; thus, the pressure difference between the PC and the ST is reduced and the depressurization that occurs in PhW2 is slower. Therefore, in PhW2, the pressure in the PC is higher for the cases with a lower pressure in PhW1. The correlation between the minor loss coefficient at the SD and the FOM remains moderate positive around 0.25 in PhW2. The ST initial temperature relationship with the FOM increases in this PhW up to around 0.90, because with a higher temperature in the ST the pressure suppression is lower so the pressure in the PC remains higher.

In the last PhW (100 – 300 s), The boiler temperature has a moderate positive correlation around 0.25, since if hotter fluid is injected, the final fluid steam temperature remaining in the PC is higher thus also the pressure. The ST initial temperature has a significant positive correlation coefficient, higher than 0.9, as at the end of the previous PhW. Therefore, the relation between this input and the FOM is almost linear.

Finally, it is possible to notice that the boiler pressure has a low correlation with the FOM for the entire duration of the transient. From this analysis it is possible to conclude that to reduce the output uncertainties it could be useful a better characterization of the localized pressure drop coefficients, in particular the SD slits and MV minor loss coefficients, since they have a significant and moderate

relationship with the FOM respectively. In addition, also the initial conditions (in particular the boiler and the ST temperatures) have a significant correlation with the FOM.

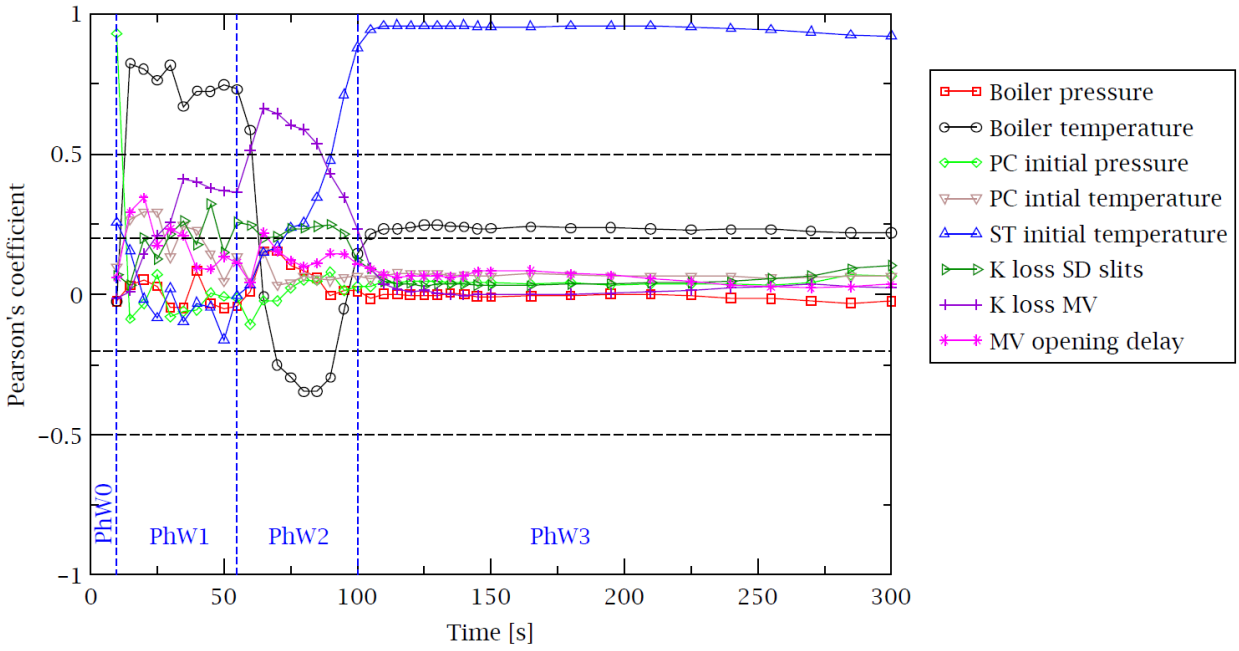

Fig. 14 Pearson's correlation coefficient

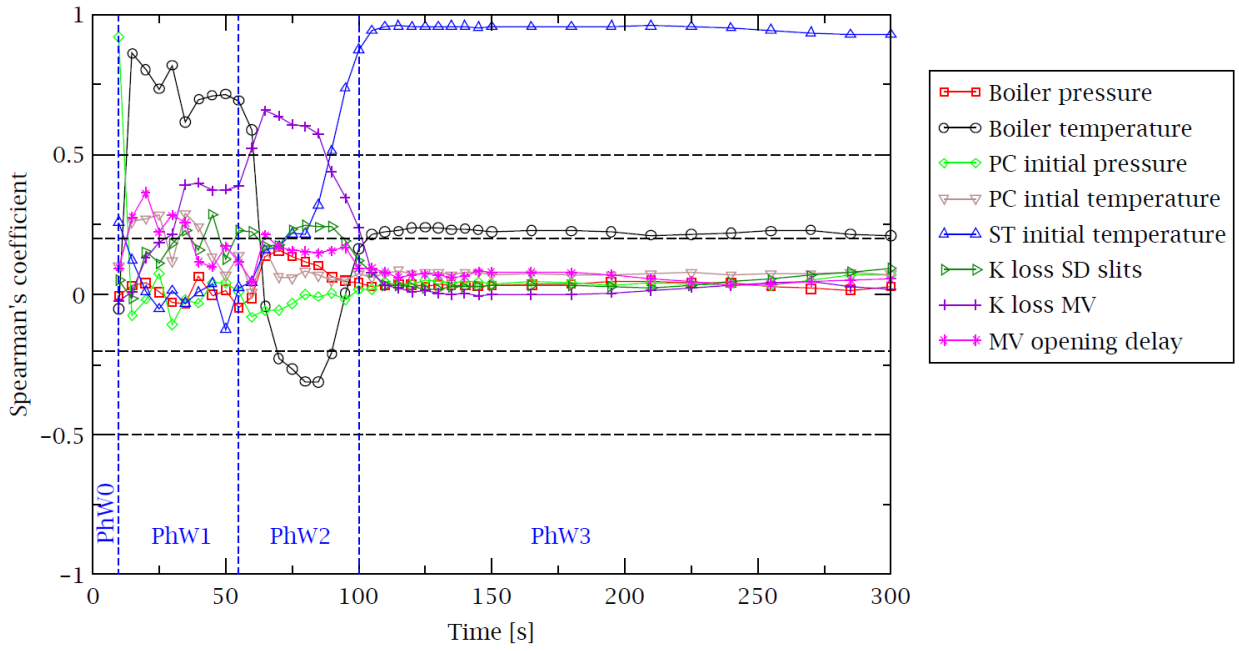

Fig. 15 Spearman's rank correlation coefficient

7. Conclusions

The ICE is one of the most important accident in tokamak type fusion reactors. The integrated ICE facility at JAERI has been built to study this event with a scaling ratio of 1/1600 with respect to ITER FEAT design.

To analyze the capability of the TRACE code to simulate the main thermal-hydraulic phenomena typical of this kind of transient, the Case4 of the experimental campaign performed in March 2000 has been considered. A TRACE nodalization of the ICE facility has been developed with SNAP and the 3D Vessel component has been used to simulate the PC, SD and VV where multidimensional phenomena could take place. The code results have been compared to the experimental one and an accuracy evaluation has been performed. The evaluation has been conducted initially in a qualitative way with the identification of the PhWs, RTPs, and the RTAs. After having assessed the capability of the code to qualitatively predict the main phenomena/processes, a quantitative accuracy evaluation has been carried out using the FFTBM. According to the reference thresholds considered, the code prediction is very good in all the PhWs.

Having qualified the nodalization and the code capability, an UA has been performed. The probabilistic method for the propagation of input uncertainties has been adopted, considering its suitability to be coupled with simulation codes. This UA has been done using the DAKOTA toolkit in a SNAP environment/architecture. Nine uncertain input parameters have been selected (with eight distributions) and the PC pressure has been chosen as FOM. With a probability content of 95%, a confidence level of 95% and only one FOM, a total of 59 code runs have been performed, based on Wilks' formula. Pearson's and Spearman's correlation coefficients have been computed to characterize the correlation between the input uncertainty parameters and the FOM selected. During the water injection phase, the parameters showing a higher correlation with the FOM are the boiler temperature and the minor loss coefficient in the SD slits. After the end of water injection, the parameters showing a higher correlation with the FOM are again the minor loss coefficient in the MV and the ST initial temperature. The MV opening delay has a moderate correlation with the FOM after the pressure set-point in the PC is reached. In addition, the results dispersion has been analyzed for five significant parameters (the PC, VV and ST pressure and the PC and VV temperature). For all the parameters the experimental data have been found to be inside the simulation dispersion band with the limited exception of the PC and VV pressures slightly underestimated by the calculations in the final part of the transient. The aim of this UA is not to be a an exhaustive uncertainty study in term of input uncertainty parameters but to develop a complete uncertainty quantification application with DAKOTA, in a SNAP environment/architecture, for a fusion reactor safety issue and to have some insights characterizing the dispersion of the results against the available experimental data and characterize the correlation between the selected input uncertainty parameters and the chosen FOM.

In conclusion, TRACE code proved to be able to simulate the main phenomena occurring in an ICE transient in a fusion like device and to predict the time dependent behavior of the most relevant parameters. The authors would like to emphasize the importance of the adopted methodology in the comparison of the calculated results and in the evaluation of the code accuracy. The use of both a qualitative and a quantitative approach is fundamental to properly assure the quality of a code calculation. In the quantitative analysis a method should be selected to quantify the error between the experimental and the calculated results as the FFTBM, adopted in the present activity. The application of the probabilistic method to propagate input uncertainties and the computation of response correlations allow to characterize the dispersion of the results and the relationship between the selected input uncertain parameters and the FOM chosen.

As a future follow-up activity for the validation of TRACE code for fusion applications, an analysis on the best modeling strategies for pressure suppression tanks is currently in progress.

Acknowledgement

The authors gratefully acknowledge USNRC for their valuable comments and suggestions during the preparation of the manuscript.

References

[1] T. Pinna, D. Carloni, A. Carpignano, S. Ciattaglia, J. Johnston, M.T. Porfiri, L. Savoldi, N. Taylor, G. Sobrero, A.C. Uggenti, M. Vaisnoras, R. Zanino, Identification of accident sequences for the DEMO plant, Fusion Eng. Des. 124 (2017) 1277-1280

[2] IAEA, ITER-FEAT Outline design report, https://www-pub.iaea.org/MTCD/Publications/PDF/ITER-EDA-DS-18.pdf (2001)

[3] K. Takase, H. Akimoto, Experimental verification of effectiveness of integrated pressure suppression systems in fusion reactors during in-vessel loss of coolant events, Nucl. Fusion 41 (2001) 1873-1883

[4] T. Kaliatka, E. Uspuras, A. Kaliatka, Modelling of Water Ingress into Vacuum Vessel Experiments Using RELAP5 Code, J. Fusion Energ. 34 (2015) 216-224

[5] K. Takase, H. Akimoto, L.N. Topilski, Results of two-phase flow experiments with an integrated Ingress-of-Coolant Event (ICE) test facility for ITER safety, Fusion Eng. Des. 54 (2001) 593-603

[6] T. Marshall, M.T. Porfiri, L. Topilski, B. Merril, Fusion safety codes: international modeling with MELCOR and ATHENA–INTRA, Fusion Eng. Des. 63–64 (2002) 243–249

[7] T. Kačegavičius, E. Urbonavičius, Modelling of ingress of coolant event into vacuum experiments with ASTEC code, J. Fusion Energy 34 (2014) 320–325

[8] G. Caruso, D. Vitale Di Maio, M.T. Porfiri, Numerical study on Ingress of Coolant Event experiments with CONSEN code, Fusion Eng. Des. 100 (2015) 443-452

[9] F. Mascari, F. De Rosa, B.G. Woods, K. Welter, G. Vella, F. D'Auria, Analysis of the OSU-MASLWR 001 and 002 Tests by Using the TRACE Code, NUREG/IA-0466 (2016)

[10] U. S. Nuclear Regulatory Commission, TRACE V5.840 Theory Manual, Field Equations, Solution Methods and Physical Models (2013)

[11] Applied Programming Technology, Inc. Symbolic Nuclear Analysis Package (SNAP) User's Manual (2012)

[12] F. Mascari, H. Nakamura, K. Umminger, F. De Rosa, F. D'Auria, Scaling issues for the experimental characterization of reactor coolant system in Integral Test Facilities and role of system code as extrapolation tool, Proceedings of 16th International Topical Meeting on Nuclear Reactor Thermal Hydraulics (NURETH-16), 6 (2015) 4921-4934

[13] W. Ambrosini, R. Bovalini, F. D'Auria, Evaluation of accuracy of thermalhydraulic code calculation, Energia Nucleare 7 (1990) 5-16

[14] H. Glaeser, GRS Method for Uncertainty and Sensitivity Evaluation of Code Results and Applications, Sci. Technol. Nuc. Ins. (2008)

[15] B.M. Adams, M.S. Ebeida, M.S. Eldred, G. Geraci, J.D. Jakeman, K.A. Maupin, J.A. Monschke, J.A. Stephens, L.P. Swiler, D.M. Vigil, T.M. Wildey, W.J. Bohnhoff, K.R. Dalbey, J.P. Eddy, J.R. Frye, R.W. Hooper, K.T. Hu, P.D. Hough, M. Khalil, E.M. Ridgway, A. Rushdi, Dakota, A Multilevel Parallel Object-Oriented Framework for Design Optimization, Parameter Estimation, Uncertainty Quantification, and Sensitivity Analysis: Version 6.7 User's Manual, SAND2014-4633 (2017)

[16] G. Caruso, M.T. Porfiri, CONSEN validation against ICE and EVITA Experimental campaign 2000 Pre-test calculations, FUS-TN-SA-SE-R-09 (2000)
[17] M. Shibata, K. Takase, H. Watanabe, H. Akimoto, Experimental results of functional performance of a vacuum vessel pressure suppression system in ITER, Fusion Eng. Des., 63-64 (2002) 217-222
[18] F. Mascari, G. Vella, B.G. Woods, K. Welter, J. Pottorf, E. Young, M. Adorni, F. D'Auria, Sensitivity analysis of the MASLWR helical coil steam generator using TRACE, Nucl. Eng. Des. 241 (2011) 1137–1144
[19] J. Staudenmeier, TRACE reactor system analysis code, MIT Presentation, Safety Margins and Systems Analysis Branch, Office of Nuclear Regulatory Research, U.S. Nuclear Regulatory Commission (2004)
[20] F. Mascari, G. Vella, B. G. Woods, K. Welter, F. D'Auria, Analysis of Primary/Containment Coupling Phenomena Characterizing the MASLWR Design During a SBLOCA Scenario, Nuclear Power Plants, InTech (2012)
[21] Office of Nuclear Regulatory Research, U.S. Nuclear Regulatory Commission, Division of System Analysis, TRACE V5.0, 2008. Theory and User's Manuals
[22] U. S. Nuclear Regulatory Commission, TRACE V5.840 User's Manual, Volume2: Modeling Guidelines (2013)
[23] A. Prošek, M. Leskovar, B. Mavko, Quantitative assessment with improved fast Fourier transform based method by signal mirroring, Nucl. Eng. Des. 238 (2008) 2668-2677
[24] A. Prošek, M. Leskovar, Use of FFTBM by signal mirroring for sensitivity study, Ann. Nucl. Energy 76 (2015) 253-262
[25] A. Prošek, JSI FFTBM Add-In 2007 User's Manual, IJS-DP-9752 (2007)
[26] F. D'Auria, M. Frogheri, W. Giannotti, RELAP/MOD3.2 Post Test Analysis and Accuracy Quantification of SPES Test SP-SB-04, NUREG/IA-0155 (1999)
[27] IAEA International Atomic Energy Agency, Best Estimate Safety Analysis for Nuclear Power Plants: Uncertainty Evaluation, Safety Reports Series (2008)
[28] A. Bersano, F. Mascari, Evaluation of a Double-Ended Guillotine LBLOCA Transient in a Generic Three-Loops PWR-900 with TRACE Code Coupled with DAKOTA Uncertainty Analysis, ATW - International Journal for Nuclear Power 11/12 (2019) 526-532
[29] https://dakota.sandia.gov/
[30] Applied programming Technology Inc., Uncertainty analyses User manual, Symbolic Nuclear Analyses Package (SNAP) (2012)
[31] S.S. Wilks, Determination of sample sizes for setting tolerance limits, Ann. Math. Stat. 12(1) (1941) 91-96
[32] S.S. Wilks, Statistical prediction with special reference to the problem of tolerance limits, Ann. Math Stat. 13(4) (1942) 400-409
[33] S.M. Bajorek, C. Gingrich, Uncertainty Methods Framework Development for the TRACE Thermal-Hydraulics Code by the U.S.NRC, OECD/CSNI Workshop on Best Estimate Methods and Uncertainty Evaluations, NEA/CSNI/R(2013)8/PART2 (2013) https://inis.iaea.org/collection/NCLCollectionStore/_Public/45/107/45107574.pdf?r=1&r=1
[34] A. Guba, M. Makai, L. Pál, Statistical aspects of best estimate method-I, Reliab. Eng. Syst. Safe. 80 (2003) 217-232
[35] Applied Programming Technology Inc., AptPlot User's Manual (2015)

[36] K.A. Gamble, L.P. Swiler, Uncertainty Quantification and Sensitivity Analysis Applications to Fuel Performance Modeling, SAND2016-4597C

[37] M.E. Stephens, B.W. Goodwin, T.H. Andres, Deriving parameter probability density functions, Reliab. Eng. Syst. Safe. 42 (1993) 271-291

[38] T. Kaliatka, E. Ušpuras, A. Kaliatka, D. Naujoks, Analysis of ingress of coolant accident in the vacuum vessel of the W7-X fusion experimental facility, EUROFUSION WPSAE-PR(16) 16324 (2016)